5-2013

Development of novel layered nanoparticles for more efficient cancer treatment.

Thomas A. Priest
University of Louisville

DEVELOPMENT OF NOVEL LAYERED NANOPARTICLES FOR MORE EFFICIENT CANCER TREATMENT

By

Thomas A. Priest
B.S. Bioengineering, University of Louisville, 2012

A Thesis
Submitted to the Faculty of the
University of Louisville
J.B. Speed School of Engineering
as Partial Fulfillment of the Requirements
for the Professional Degree

MASTER OF ENGINEERING

Department of Bioengineering

May 2013

DEVELOPMENT OF NOVEL LAYERED NANOPARTICLES FOR MORE EFFICIENT CANCER TREATMENT

Submitted by: _____
Thomas A. Priest

A Thesis Approved On

_____
(Date)

By the Following Reading and Examination Committee:

_____
Hermann B. Frieboes, Ph.D, Thesis Director

_____
Andrea S. Gobin, Ph.D

_____
Stuart J. Williams, Ph.D

ACKNOWLEDGEMENTS

I would like to thank all of the people working in the research group of Dr. André Gobin for helping me with some of the lab work involved in this project, as well as answering questions and providing insightful feedback.

Dr. André Gobin

Dr. Guandong Zhang

Kurtis James

Dhru Patel

I would also like to thank Dr. Hermann Frieboes for accepting me as a student during a time of difficult faculty turnover. It is difficult to manage several students while maintaining an active research presence, teaching classes, and mentoring undergraduates, but he can manage it all expertly.

I would also like to thank Chris England. This work was in many ways a strong collaboration with Chris to assist in all of the work that he is performing. I wish you luck in your doctorate program.

And finally, I would like to thank Tanya Trump, for providing me with support and encouragement to complete my thesis. You are a great inspiration, and thank you for sticking by me, I know I can be difficult.

ABSTRACT

Cancer is the second-most leading cause of death in the United States, with 1.66 million new cases expected to be diagnosed and over 580,000 Americans expected to die of cancer in 2013 alone. (American Cancer Society 2013) Current treatments result in damage to the healthy tissues and incomplete resections of solid tumors, but by harnessing nanotechnology, more effective treatments can be constructed. Gold nanoshells present a promising option for targeted cancer therapy. The anatomy of tumors causes the "enhanced permeability and retention" effect, which means that nano-scale particles will extravasate from the bloodstream and accumulate in the tumors. However, small nanoparticles must still diffuse from the tumor vasculature into the tumor tissue. Due to impaired vascularization, the particles are unable to reach into the entire tumor region. The purpose of our project is to create a "two-layer" nanoshell coated with alkanethiol and phosphatidlycholine and a "three-layer" nanoshell that coats the "two-layer" system with a layer of high-density lipoprotein. It is proposed that these coatings will allow for better penetration of solid tumors compared to the standard nanoshells modified with poly(ethylene glycol) (PEG). In addition to the nanoshells, citrate-gold nanoparticles were investigated as a control. Size, zeta potential, and morphology were optimized, and the penetration of the particles into solid tumors was investigated using dark-field microscopy. It was discovered that the "two-layer" nanoshells exhibited significantly more uptake into the solid tumors compared to PEGylated nanoshells, and should be further investigated as a platform for targeted cancer therapies.

TABLE OF CONTENTS

LIST OF FIGURES

I. INTRODUCTION

Cancer is the second most common cause of death in the United States, (American Cancer Society 2013) with an estimated 580,000 Americans dying of cancer in 2013 alone. (American Cancer Society 2013) There are also an estimated 1,660,000 new cancer diagnoses expected this year. (American Cancer Society 2013) While advances in early diagnostics and treatment methods have increased the five-year survival rate to 68% for 2002 – 2008, more advances in treatment methods are necessary to effectively treat cancers and further raise the survival rates. (American Cancer Society 2013) The application of nanotechnology to better deliver therapeutic agents to the tumor regions has attracted a vast amount of research. Solid tumors have several characteristics that differ from healthy tissue, including excessive angiogenesis. Nanoparticles and drugs on the nano scale (60 – 400 nm) exhibit increased extravasation into the interstitial space of solid tumors due to a passive mechanism termed the "enhanced permeability and retention" (EPR) effect. (Kong, Braun et al. 2000, Maeda 2001) While the concept seems trivial, the targeted delivery of anticancer drugs (targeted chemotherapy) using nanoparticles is a major research goal. Targeted treatments both increase the effectiveness of the drugs while simultaneously reducing the systemic toxic side effects to the patient. However, there are many factors that dictate the effectiveness of a nanoparticle system in reaching the tumor regions within a patient. The particle size, surface charges, and morphology all contribute to the pharmacodynamics and cytotoxicity of the nanoparticle system. (Murphy, Gole et al. 2008, Zamboni, Torchilin et al. 2012) These properties must be tailored in order to design a nanoparticle system that exhibits optimal depths of penetration into solid tumors.

Gold nanoparticles have exhibited some of the more promising research in recent years. Bulk gold itself is an inert material, though gold nanoparticles smaller than 5nm in diameter have documented cytotoxic properties. (Alkilany and Murphy 2010, Kennedy, Bickford et al. 2011) However, larger particles have been demonstrated to display little cytotoxicity, depending on the surface charge. Cationic particles are more cytotoxic at lower concentrations compared to anionic nanoparticles; this has been attributed to electrostatic interactions of the positively-charged particles with the negatively-charged cell membrane. (Goodman, McCusker et al. 2004) In addition, surface coatings of poly(ethylene glycol) (PEG) effectively "mask" the nanoparticles from the immune system, further lowering cytotoxicity. (Murphy, Gole et al. 2008, Kennedy, Bickford et al. 2011)

The major advantages of a gold nanoparticle system are the relative ease of synthesis and the tunable nature of the optical properties of the nanoparticles. The Turkevich method has been used to synthesize colloidal gold for many years, and results in nanoparticles with a narrow size distribution that is easily tunable based on the ratio of the reactants. (Frens 1973) A sharp absorption profile is observed in the 520 – 540 nm range. (Turkevich, Stevenson et al. 1951, Frens 1973, Turkevich 1985) The optical properties of gold nanoparticles prepared via the Turkevich method can only be tuned to a limited degree. However, gold nanoshells, which consist of a silica core coated with a thin layer of gold, exhibit easily tunable optical properties and can be applied as imaging contrast agents (Loo, Lowery et al. 2005), therapeutic agents (Gobin, Watkins et al. 2010), or combined imaging and therapeutic agents (Gobin, Lee et al. 2007). By varying the thickness of the silica core or the gold shell, the peak absorption profile can be

selected, from infrared through the spectrum of visible light. (Oldenburg, Averitt et al. 1998) Early work with gold nanoshells produced a system coated with poly(vinyl alcohol) (PVA) that exhibited a peak absorption at 800 nm, in the near-infrared (NIR) region of light. (Oldenburg, Jackson et al. 1999) Near-infrared light is not considered harmful when directed at tissues, as the heating effect is very minimal. (Ito, Kennan et al. 2000) However, as metallic particles absorb wavelengths of light, they begin to resonate, releasing the energy as heat. To apply this concept to cancer therapies, PEGylated gold nanoshells were coupled with a NIR-emitting laser. The combination of nanoshells and NIR treatment effectively caused irreversible tissue damage to solid tumors *in vivo* due to sustained hyperthermia, while NIR treatment alone did not result in any adverse effects. (Hirsch, Stafford et al. 2003) Current clinical trials are underway, testing the efficacy of the gold nanoshell-mediated hyperthermia treatments. (Pilot Study of AuroLase Therapy 2013)

A. PURPOSE OF THE RESEARCH

NIR-absorbing gold nanoshells are proven to be effective at killing solid tumors due to hyperthermia when treated with a NIR laser. However, the nanoshells have been PEGylated in all previous investigations of their potential. Phosphatidlycholine (PC) has been used as a passivating agent for gold nanorods, significantly reducing their cytotoxicity. (Takahashi, Niidome et al. 2006) In addition, PC is the most abundant phospholipid within the body and can be found in all cell membranes. The structure of PC is depicted in Figure 1. (Avanti Polar Lipids 2013) When forming a lipid bilayer, the

negatively charged phosphate groups are oriented on the outside of the layer, resulting in an anionic surface charge.

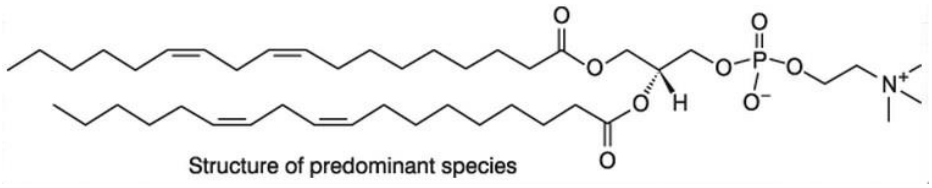

Figure 1 – Structure of L-α-phosphatidlycholine isolated from soybeans.

In order to form a layer of PC around the gold nanoshells, a hydrophobic layer must also be created. Thiol groups exhibit strong binding to gold, and can be used to displace other stabilizing ligands and adsorbed molecules to stabilize the particle. An alkanethiol possesses the optimal qualities for this; the hydrophobic carbon chains will interact with the fatty acids of the PC to form a properly oriented layer. This "two-layer" approach was theorized to display better biocompatibility and thus better penetration into solid tumors when compared to PEGylated particles. With the "two-layer" method, a hydrophobic region is created between the PC and alkanethiol, which could potentially hold hydrophobic drugs to produce a more potent therapeutic agent.

A "three-layer" method was also developed; evidence suggests that high-density lipoprotein (HDL) uptake in hepatocytes is upregulated in liver cancers. (Jiang, Nilsson-Ehle et al. 2006) Adding a layer of HDL around the "two-layer" particles could potentially allow the particles to penetrate more deeply into liver cancers as the surface modifications make uptake by the hepatocytes more likely rather than just relying on the EPR effect to passively accumulate particles within solid tumors.

The purpose of developing the "two-" and "three-layer" nanoshells are to directly compare the penetration of the particles into solid tumors to the current standard, the

PEGylated AuroShells™. In addition, the depth of penetration of "two-layer," "three-layer," and PEGylated citrate-gold nanoparticles are also compared to the nanoshells. While citrate-gold nanoparticles are much smaller than the silica-core gold nanoshells, they do not exhibit absorption in the NIR range and cannot be used for photothermal ablation therapy.

This study is focused on identifying the number of particles within the solid tumors at varying depths of penetration. By accurately counting the amount of particles within specific regions of tissue, a diffusion gradient can be constructed and combined with mathematical modeling to better understand the effectiveness of these particles for cancer treatment. The experimental results can then be utilized to calibrate the complex computational simulations involved with the dynamics of solid tumor interactions. (van de Ven, Wu et al. 2012)

II. PROCEDURE

A. SYNTHESIS OF SILICA-CORE GOLD NANOSHELLS

Gold nanoshells were prepared according to previously established methods. (Gobin, Lee et al. 2007)

i. SYNTHESIS OF SILICA CORES

The silica cores were grown according to the Stöber process, using tetraethyl orthosilicate (TEOS) in ethanol. (Stöber, Fink et al. 1968) A round bottom flask was filled with 225mL 200proof ethanol, and the liquid was stirred. 12.5mL of fresh ammonia was then added to the ethanol to provide the basic environment required for the reaction to proceed. Three minutes after the addition of ethanol, 7.5mL of TEOS was added to the flask, and the mouth of the flask was immediately covered with paraffin. After reacting for 24 hours, the paraffin was removed from the mouth of the flask to allow the excess ammonia to evaporate. The completed silica cores measure approximately 110nm in diameter, on average.

ii. APTES MODIFICATION OF SILICA CORES

The silica cores were modified by coating with aminopropyltriethoxysilane (APTES). Prior to modification, 15mL of silica cores were placed in a 50mL polypropylene tube and centrifuged at 1500xg for 20min. The supernatant was then removed, and the pellets combined. The tubes were then washed with ethanol and sonicated for 20 min prior to centrifugation at 1200xg for 20 min. All of the pellets were combined again, and the silica cores were dispersed in 40mL of 160 proof ethanol. 4%

APTES was added to the silica cores, and solution was sonicated for 120 min at elevated temperature, before being placed on the rocker bed for 20 hours.

The cores were then centrifuged at 1000xg for 20 min, and the supernatant discarded. The pellet was resuspended in 50% ethanol (in dH_2O) and sonicated for 20 min. The washing step was then repeated to finish the modification of the silica cores.

iii. SYNTHESIS OF THPC COLLOID

A gold colloid solution was also prepared, in order to coat the completed silica cores. (Duff, Baiker et al. 1993) A stock solution of the reducing agent for the colloidal gold was prepared. 0.4mL of tetrakis(hydroxymethyl)phosphonium chloride (THPC) was added to 33mL of distilled H_2O (dH_2O) and stirred for approximately 5 minutes. A 500mL plastic beaker was then filled with 180mL of cold dH2O. To this solution, 1.2mL of 1M NaOH and 4mL of the THPC stock solution were added while stirring. Finally, 6.75mL of 1%/wt HAuCl4 in dH2O was quickly added to the solution, and after 1 minute of agitation, the reaction was halted. The THPC-gold colloid solution was then stored in a 275mL plastic flask at 4°C. The THPC-gold colloid was aged at 37°C for at least 4 days prior to use in order to ensure proper colloid growth and concentrated 10x via rotary evaporation before use.

iv. NANOSHELL SEED FORMATION AND GOLD SHELL REDUCTION

In a 50mL polypropylene tube, 20mL of concentrated THPC colloid was reacted with the APTES-modified silica cores and sonicated for 60 min. The reaction was then allowed to progress for 48 hours. The solution was then centrifuged at 600xg for 20

minutes and the pellet collected. The pellets were combined and resuspended in 20mL dH_2O, then centrifuged again at 600xg for 20 minutes. The pellet was then resuspended in 20mL dH_2O, and the optical intensity of the seeds was measured via UV-vis spectroscopy. The seeds were diluted an optical density (OD) of 0.5 at 530nm. A K_2CO_3-$HAuCl_4$ (KCarb) solution was prepared by combining 50mg K_2CO_3 with 200mL dH_2O and 3mL 1% wt/v $HAuCl_4$. A sweep of the seeds was performed to optimize the reaction amounts of KCarb, seeds, and formaldehyde (the reducing agent) for the final gold shell reduction in order to produce the most desired optical properties. The seeds were then mixed with optimal amounts of KCarb and formaldehyde to complete the gold nanoshells.

B. SYNTHESIS OF CITRATE-STABILIZED GOLD NANOPARTICLES

Colloidal gold nanoparticles were also prepared according to published methods. The particles were formed according to a modified Turkevich synthesis. (Turkevich, Stevenson et al. 1951, Frens 1973) A stock solution of 1%/wt $HAuCl_4$ in distilled H_2O was prepared. This stock solution was diluted to 0.01%/wt HAuCl4, and 200mL was added to a 250mL Erlenmeyer flask. The solution was then brought to a boil in a water bath under vigorous stirring, and kept boiling for 10 minutes. A 2.3mL solution of 1%/wt sodium citrate in distilled H_2O was added to the boiling gold solution, and the reaction was carried out for approximately 15 minutes while boiling. The reaction solution shifted colors from pale yellow to a red/reddish-purple color, indicating that the conversion of ionic gold into colloidal gold had been achieved. The solution was then cooled to room temperature, and concentrated to 20mL using a rotary evaporator.

C. SURFACE MODIFICATIONS OF PREPARED PARTICLES

Both the prepared nanoshells and citrate-gold nanoparticles were modified to produce "two-layer," "three-layer," and PEGylated particles.

i. MODIFICATION WITH POLY(ETHYLENE GLYCOL)

The prepared particles were modified with poly(ethylene glycol) (PEG) to form the control group. PEGylated particles have been shown to have stealth properties with the immune system. (Gobin, Lee et al. 2007) The optical density of the nanoparticles was determined using absorbance spectroscopy, measuring wavelengths from 400 – 1100nm. 1μL of a 20mM PEG-thiol solution was added for every 1 OD/mL of the particle solution. The gold-sulfur bond forms spontaneously, and is a very strong bond. The sample was then sonicated for 10 minutes, and left on a rocker plate overnight. The PEGylated particles were then centrifuged at 300xg for 15 minutes to separate the excess PEG. The supernatant was removed, and the pellet collected and redispersed in dH_2O to the optimal optical density.

ii. "TWO-LAYER" PARTICLE MODIFICATION

"Two-layer" particles were formed by first modifying the particles with an alkanethiol. Two 50mL polypropylene tubes were each filled with 25mL of ethanol containing 100uL of hexadecanethiol. To each of these tubes, 10mL of the

nanoshell/citrate-gold nanoparticle solution was added. The tubes were then sonicated for 60 minutes, and left overnight on a rocker plate. As the sulfur of the alkanethiol reacts with the gold surfaces and spontaneously forms strong gold-sulfur bonds, the particles become hydrophobic, creating a film on the sides of the tubes and on the surface of the liquid. The solutions were centrifuged at 300xg for approximately 14 minutes, in order to form a pellet. The supernatant was then removed, and the tube washed with 20mL ethanol before a second centrifugation at 300xg for 14 minutes. The supernatant was removed again, and the tubes were left to air dry. Once the ethanol evaporated from the tubes, 10mL $CHCl_3$ was added to each tube. $CHCl_3$ is an organic, slightly polar solvent, and the hydrophobic thiol-stabilized particles are soluble in the solvent. The tubes containing thiol-stabilized particles in $CHCl_3$ are then sonicated for 60 minutes to ensure that the particles are redispersed.

After sonication, 150uL of 25mg/mL soy phosphatidlycholine (PC) in $CHCl_3$ was added to the tubes, which were then left on the rocker plate overnight. The hydrophobic tails of the PC interact with the exposed carbon chains of the particles, forming a complete layer of PC around the particles, causing them to become hydrophilic as only the polar headcaps of the phospholipid are exposed in solution. Once the PC has coated the particles, the solution was placed into glass test tubes and dried under air to allow the $CHCl_3$ to evaporate. Once tubes were dry, the particles were redispersed in 5mL dH_2O and sonicated for 60 minutes and combined in. In order to remove the particles that were not fully coated with PC, the solutions were centrifuged at 300xg for 15 minutes. The supernatant was removed and collected, and the tube was then washed with dH_2O before a second centrifugation step at 300xg for 15 minutes. The supernatant was collected

again, and the collected supernatant combined and placed in a new 50mL polypropylene tube. The "two-layer" (thiol-PC) particles are complete at this stage, and an aliquot was taken for characterization by absorbance spectroscopy, DLS and SEM. The desired optical density (OD) of the particles was then reached by diluting the sample with dH_2O.

iii. "THREE-LAYER" PARTCLE MODIFICATION

The "three-layer" (thiol-PC-LP) particles were then prepared by the addition of high-density lipoprotein (LP) derived from human plasma to the completed "two-layer" particles. The LP sticks to the surface layer of the "two-layer" particles, and potentially becomes interspersed within the phosphatidlycholine layer. To a 4.5mL sample of the "two-layer" particles, 3mg LP was added per 20OD. The solution was then sonicated for 10 minutes and left overnight at 4°C. An aliquot was taken for characterization by absorbance spectroscopy, DLS and SEM, and the completed "three-layer" particles were diluted to the desired optical density with dH_2O.

D. INCUBATION OF PARTICLES WITH TUMOR SPHEROIDS

Spheroids comprised of cancer cells from three different cell lines were utilized to test the diffusion of the different particle compositions and modifications. HEPG2 (liver hepatocellular carcinoma), A549 (human lung adenocarcinoma), and S2VP10 (pancreatic metastatic adenocarcinoma) spheroids were incubated with 40 uL particles at 25 OD. The spheroids typically measured between 0.5 and 2 mm in diameter, though the S2VP10 cells produce small, grape-like bunches and do not form proper spheroids. These cell

lines were chosen due to the hypoxic regions within the center of the tumors, which gives rise to necrosis of the cancer tissues. The cells were incubated with the particles for six hours before being washed with PBS, in order to ensure particle penetration into the spheroids. The spheroids were then placed in the cryomolds made of tissue freezing medium. The samples were allowed to dry for two hours, and the sectioned at 5μm using a Lecia CM1860 Cryostat. The sectioned spheroids were then fixed onto Superfrost Plus microscope slides. The successful fixation of the spheroid to the slide was determined via bright-field microscopy. Excess media was removed from the slides by soaking with 30% Neutral Buffered Formalin for 1 minute. The slides were then washed in DI water prior to analysis.

E. CHARACTERIZATION OF PARTICLE PROPERTIES

The prepared particles were analyzed with scanning-electron microscopy (SEM), zeta-potential analysis, and UV-vis absorbance spectroscopy in order to determine the characteristics of the particles.

A Zeiss Supra 35VP SEM was used to characterize size and morphology of the particles. An aliquot of the prepared particles was taken in order to perform absorbance spectroscopy and zeta-potential analysis. 100μL of the particles was diluted with 900 μL of dH2O in order to form a 10x dilution of the original sample. This dilution was then placed in a clear, plastic 1 cm cuvette, which was inserted into a Varian Cary 50 Bio UV-Visible Spectrophotometer. The sample was scanned from wavelengths of 400 – 1100 nm. The wavelength of the peak absorbance recorded and the measured peak absorbance

multiplied by a factor of 10 to determine the optical density of the sample. The OD was used to determine the optimal amounts of layering agents needed during the synthesis of the modified particles. The sample was then transferred to a Malvern Zetasizer Nano ZS90 for automated zeta-potential analysis with the Malvern software tools.

F. OPTICAL ANALYSIS VIA DARK-FIELD MICROSCOPY

An Olympus BX43, fitted with a condenser from Cytoviva, was utilized for the dark-field microscopy. Images were captured at 60x magnification using a Dage XLMTC optical camera. The system is depicted in Figure 2. The samples were prepared again by soaking in cold acetone, 10% neutral buffer formalin, and dipping in dH_2O. Once the slides were dried, the region around the tissue was identified by bright-field microscopy and marked for ease of identification. A drop of oil was placed on the slide and a coverslip attached. A drop of oil was then placed on the condenser, and the condenser was brought into contact with the slide. The light source was focused and aligned at 10x magnification in order to produce the best quality images. Another drop of oil was placed on top of the coverslip, and an oil-immersion 60x magnification objective was then focused.

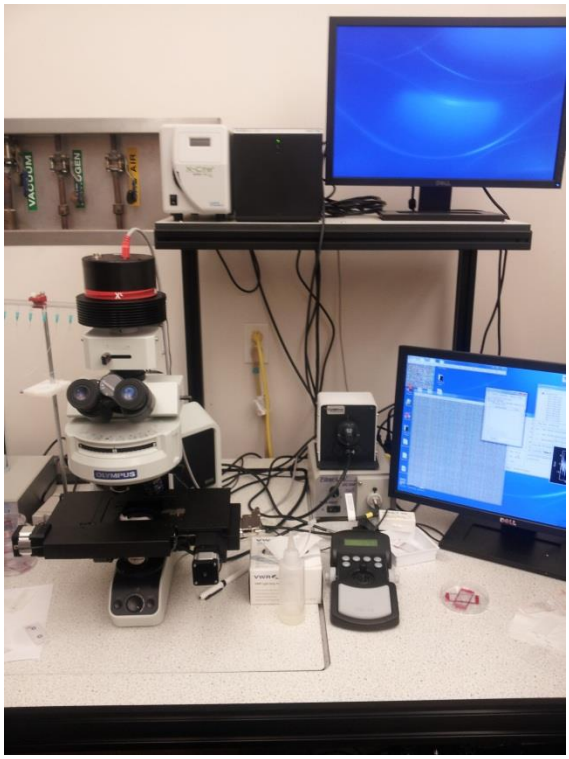

Figure 2 – Setup of the Olympus BX43 microscopy system.

Images were captured at 12-bit resolution at a size of 2048x2048 pixels using Dage Xponent7. At a magnification of 60x, a distance of 1um measured to 8.1 pixels. However, given the light-scattering properties of the nanoparticles, they appear larger than their actual size and are easily identified, especially when forming aggregated complexes. All image analysis was performed using NIH ImageJ. An automatic filtering algorithm was applied to all images, which separated out the majority of the particles from the background of tissue. (Yen, Chang et al. 1995) To ensure that no particles were inadvertently filtered, measurements were taken utilizing both the original and the filtered image simultaneously.

Images of nanoparticles alone were used to determine the average appearance of size of the nanoparticles. A known area of the image was measured, and the region-of-

interest (ROI) intensity was recorded. The number of particles was then manually counted, and the ROI intensity was divided by the particle count in order to determine the average size particle.

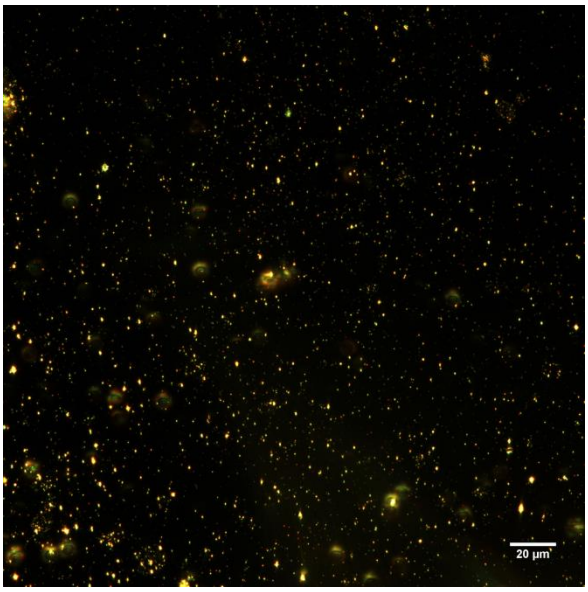

Figure 3 – Dark field image of "two-layer" nanoshells.

The number of particles present within a given area was then manually counted, using this average particle size for reference in order to form a reasonable estimate in the case of aggregated particles within the tissue. Regions located at varying depths of penetration from the periphery of the spheroid were analyzed on each image in order to visualize the diffusion gradient of the nanoparticles into the center of the cancer tissues. The results were then compared internally to determine if a particular particle composition and surface modification penetrated the tissue more easily.

V. RESULTS AND DISCUSSION

The nanoparticles were characterized with UV-vis absorbance spectroscopy, zeta potential analysis, and scanning electron microscopy to ensure that proper particle formation and modification was achieved.

The optical and charge measurements are displayed in Figure 4, and indicate that all of the surface modifications were successful. Prepared citrate-gold nanoparticles (A) had a peak absorbance of 535nm, which is consistent with literature. (Kimling, Maier et al. 2006) The silica-gold nanoshells (B) exhibited peak absorbance at 810nm. The nanoshells demonstrated ideal optical properties for use in near-infrared experiments (O'Neal, Hirsch et al. 2004, Gobin, Lee et al. 2007), though NIR treatments were not included in the scope of this work. In order to verify the surface modifications of the nanoparticles, the zeta potential was measured. Surface modification with phosphatidlycholine and thiol result in more highly negatively charged particles compared to PEGylated particles. Conversely, the high-density lipoprotein causes the zeta potential of the particles to become more positively charged when compared to PEGylated particles, but still results in slightly negatively charged particles. The measured zeta potential of all particle types is displayed in (C). The PEGylated citrate gold nanoparticles exhibited a zeta potential of -9 mV, while the “two-layer” citrate gold nanoparticles had a zeta potential of -20 mV and the “three-layer” citrate gold nanoparticles -2 mV. The gold nanoshells exhibited consistently higher surface charge than the citrate gold nanoparticles, which is consistent with the larger size of the nanoshells. PEGylated nanoshells had a zeta potential of -18 mV, “two-layer” nanoshells

measured a zeta potential of -29 mV, and the "three-layer" nanoshells a zeta potential of -6.8 mV.

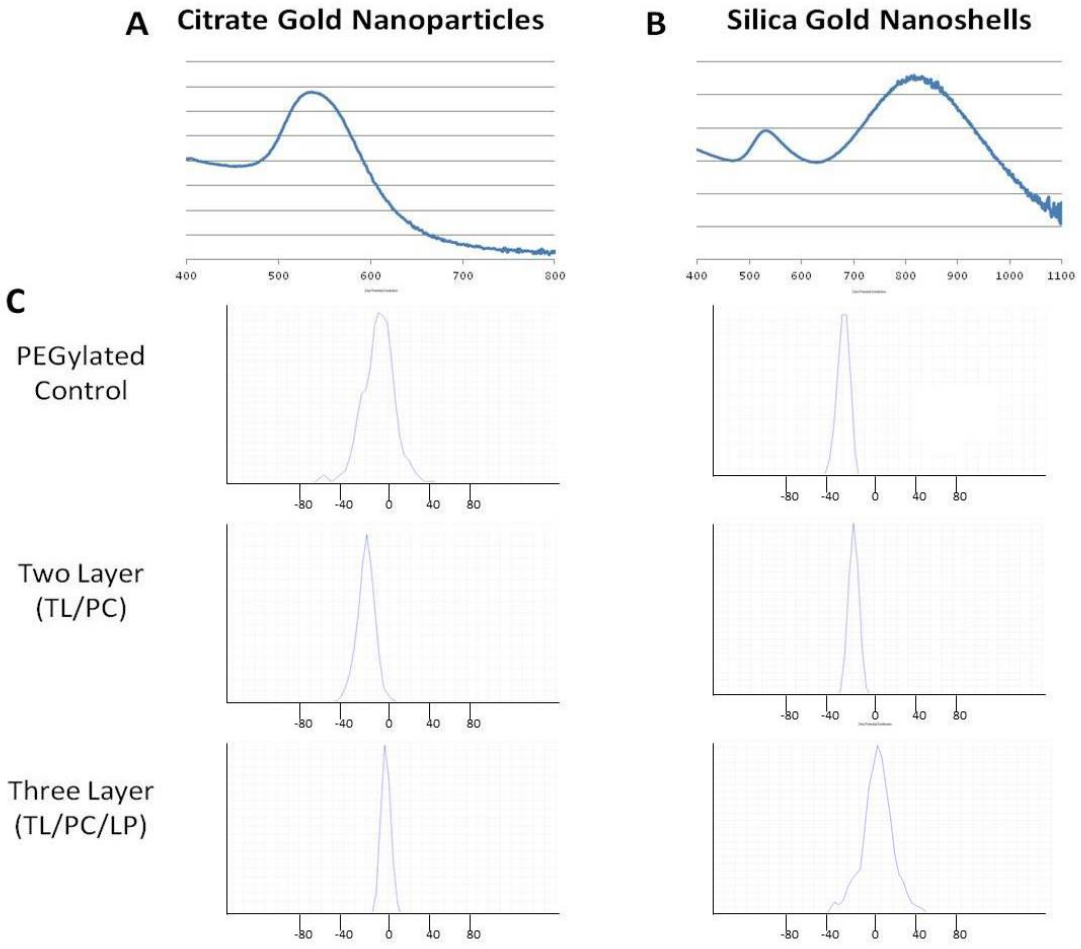

Figure 4 - Characterization of the Citrate Gold Nanoparticles and Gold Nanoshells by UV-Visible Spectrometry and Zeta Potential Analysis.

Scanning electron microscopy (SEM) was used to determine the size and morphology of the particles (Figure 5). The shape of nanoparticles has been demonstrated to affect the particle uptake into tissues. (Kennedy, Bickford et al. 2011) Both the citrate-gold nanoparticles and gold nanoshells are spherical, which is desired to produce the most optimal optical properties for future NIR treatments. However, the

citrate gold nanoparticles exhibited some irregular morphology, and were not always spherical.

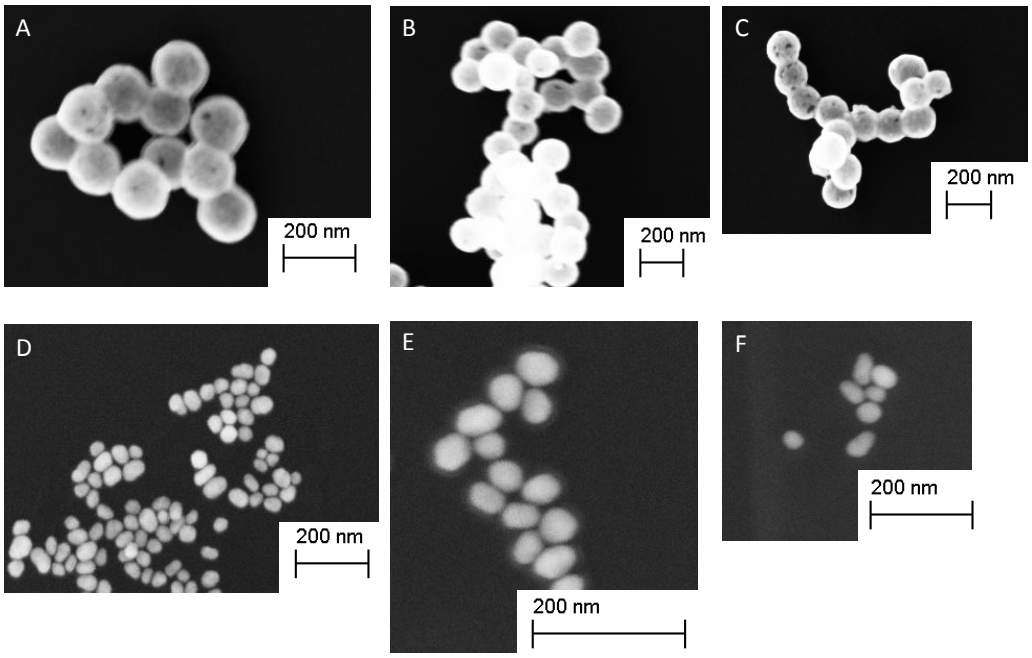

Figure 5. Scanning Electron Images of Functionalized Citrate-Gold Nanoparticles and Gold Nanoshells. (England et al., in prep.)

The PEGylated gold nanoshells (A) have spherical morphology and are ~150nm in diameter. The addition of organic compounds onto the surface of the gold nanoshells is evidenced by a "halo" effect around the particles for both the "two-layer" (B) and "three-layer" (C) particles. Citrate gold nanoparticles are much smaller than nanoshells, measuring ~50nm in diameter. Aggregation was more prevalent with citrate gold nanoparticles, as evidenced by the PEGylated particles (D). This aggregation is due to the decreased zeta potential of citrate gold nanoparticles when compared to the gold nanoshells. The "two-layer" (E) and "three-layer" (F) nanoparticles also exhibited the "halo" effect, indicating the presence of organic material on the surface of the particles. The addition of hexadecanethiol and PC added roughly 10 nm to the diameter of gold

nanoshells and LP added another 10 nm to the diameter. There was no measurable size difference between the modified citrate gold nanoparticles. The evidence of the "halo" around the modified particles and the measured increase in size further indicates the successful surface modifications of the particles.

Modified particles within the sectioned spheroids were observable in the images captured via dark-field microscopy. The particles reflected the light, displaying sharp contrast with the surrounding tissue, and could be easily counted. A representative image is displayed in Figure 6, and the arrows pointing to the small red-orange dots indicate the position of some particles within the tissue.

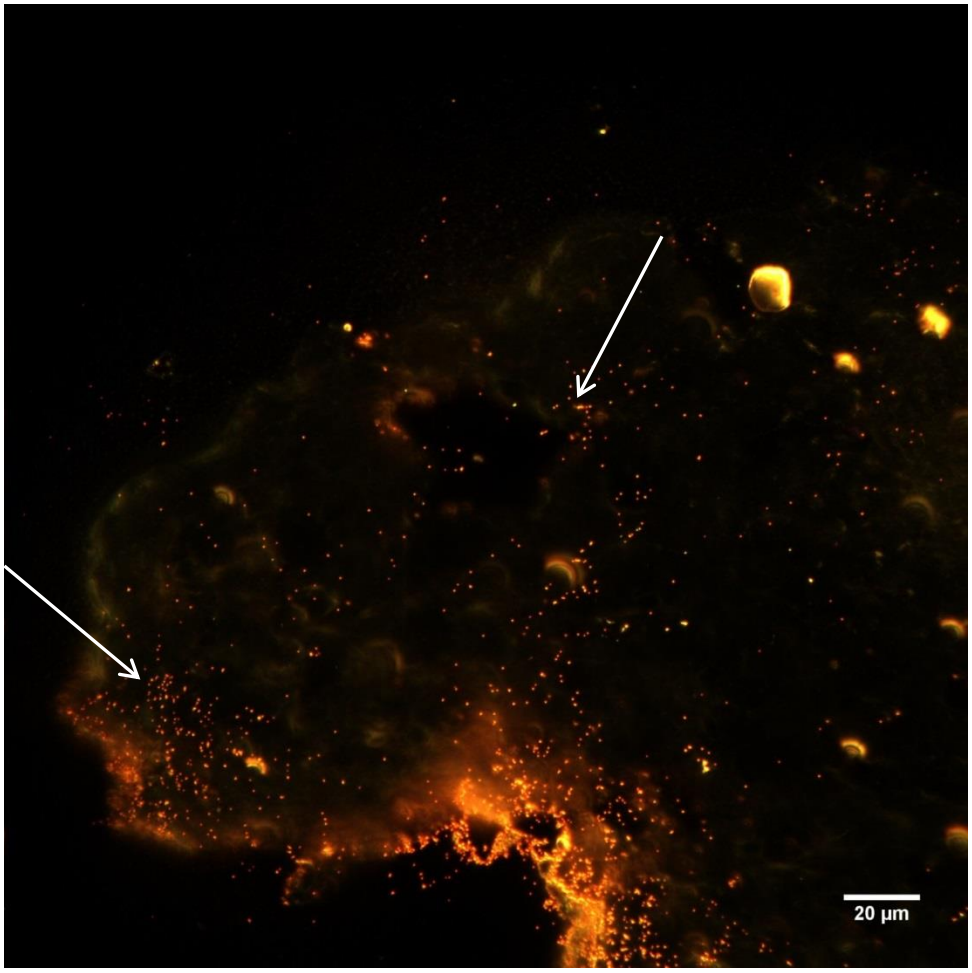

Figure 6 – Dark-field image of A549 spheroid incubated with gold nanoshells.

However, to ensure that the particles could be distinguished from the tissue, the images were filtered to remove the background via the Yen algorithm. (Yen, Chang et al. 1995) The images were considerably clearer after the algorithm was implemented, but particles were counted using the filtered and unfiltered images simultaneously to ensure that there were not particles inadvertently removed from the count. (Figure 7)

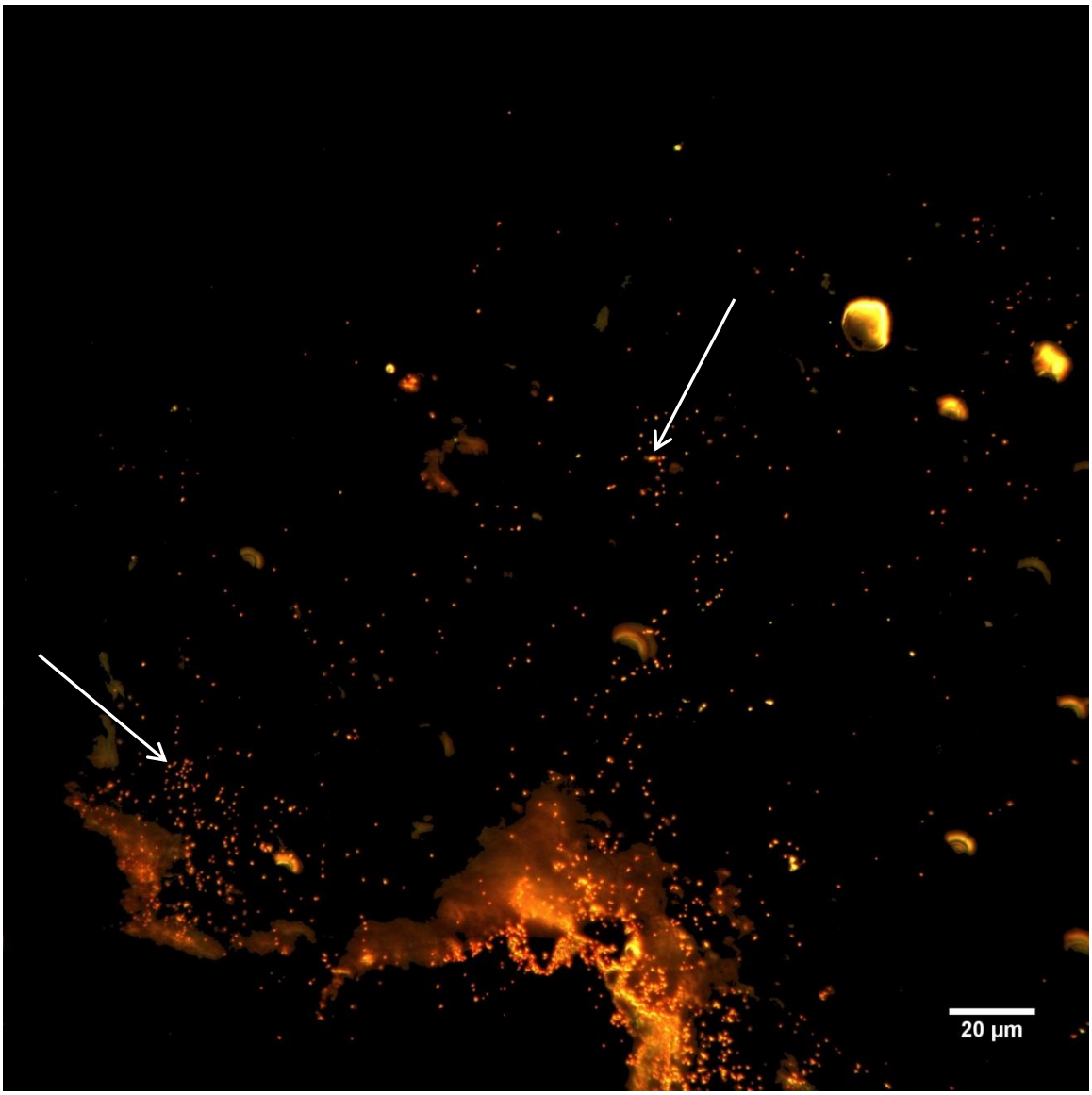

Figure 7 – Dark-field image of A549 spheroid, filtered using the Yen algorithm.

The uptake and diffusion of particles from the periphery of the tumor spheroids into center regions was analyzed via the obtained particle counts from the dark-field images, and presented in Figure 8. The left column lists the citrate-gold nanoparticles, while the right column displays the gold nanoshells. The three different cell lines that comprise the spheroids are listed on the left of the graph. The control particles (PEGylated particles) are represented by black diamonds, while the "two-layer" particles are represented by gray square and "three-layer" particles by a dark gray triangle.

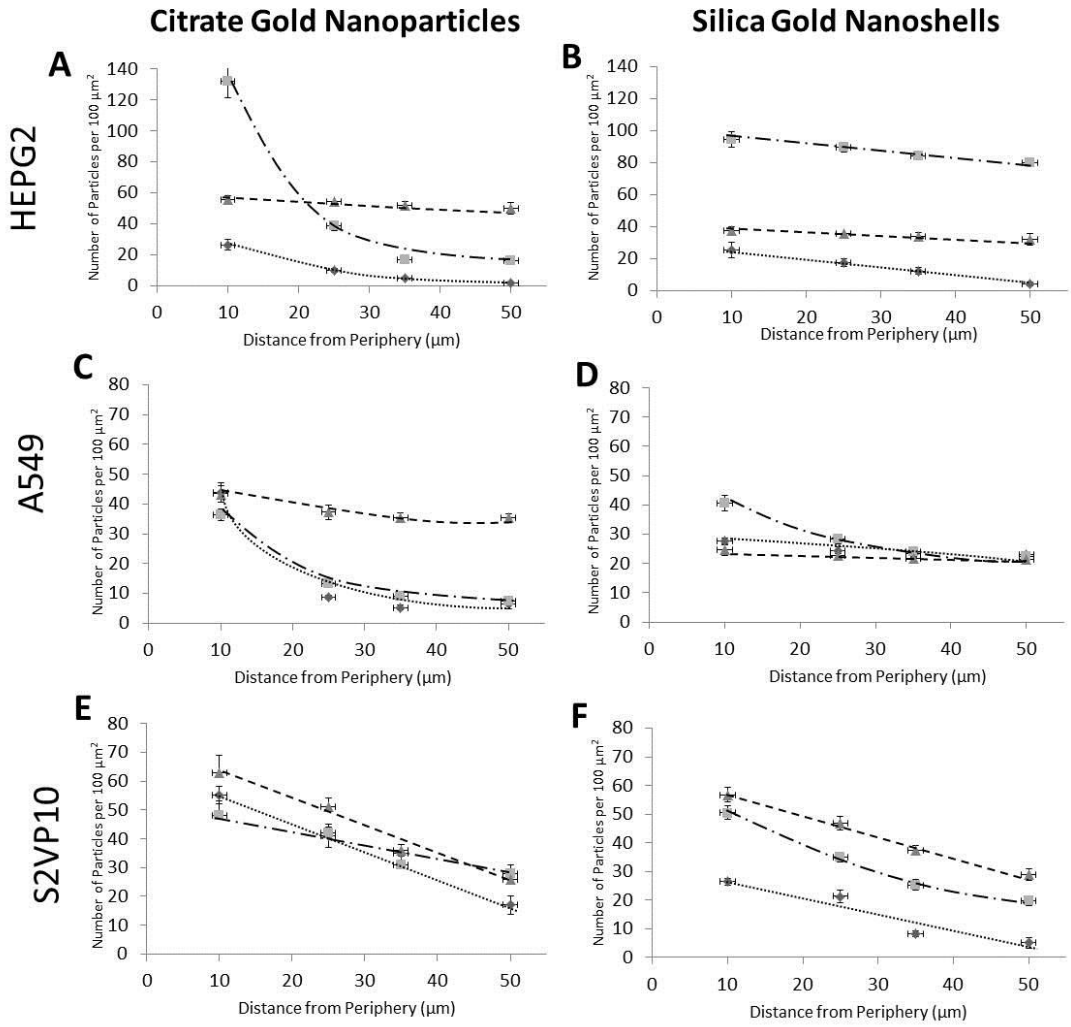

Figure 8 – Nanoparticle Diffusion into Center Regions of the Spheroids. PEGylated: Diamond; "Two-layer": Square; "Three-layer": Triangle. (England et al., in prep.)

The measured amount of particles penetrating the spheroids was generally highest for the "two-layer" particles. However, the "three-layer" particles showed slightly higher penetration into S2VP10 spheroids, but this could be due to the unique morphology of S2VP10, which resembles a cluster of grapes, and other cancer-specific interactions with the high-density lipoprotein. There were no instances where the PEGylated particles displayed higher particle penetration into the spheroids compared to "two-layer" or "three-layer" particles. Citrate-gold nanoparticles exhibited approximately 28% more particle penetration at the spheroid periphery compared to the gold nanoshells, but this is mostly due to the larger size of the gold nanoshells. Gold nanoshells are three-times the size of the citrate-gold nanoparticles. While the number of particles is lower for gold nanoshells, their application for cancer therapy is much greater than citrate-gold nanoparticles. Gold nanoshells possess tunable optical properties, and photothermal treatment has shown to reduce cell viability significantly. (Lowery, Gobin et al. 2006, Gobin, Lee et al. 2007) Internally comparing the gold nanoshell results across spheroid types, the "two-layer" nanoshells exhibited an average 51% more penetration into the spheroids compared to "three-layer" nanoshells. Both the "two-layer" and "three-layer" nanoshells outperformed PEGylated nanoshells, the current standard, handily. "Two-layer" nanoshells demonstrated a staggering 325% increase in measured particle penetration compared to the current standard, and "three-layer" nanoshells displayed an increase of 173% compared to the PEGylated nanoshells. Rather than PEGylating gold nanoshells, modifying the nanoshell with an alkanethiol and phosphatidlycholine creates a viable "two-layer" nanoshell platform that consistently outperforms the current standard when measuring particle uptake. As such, "two-layer" nanoshells should be further

considered for potential photothermal and targeted drug delivery therapies in the fight against cancer.

IV. RECOMMENDATIONS

The work can be continued by examining the efficacy of the "two-layer" nanoshell system in photothermal applications and determining its benefits compared to PEGylated nanoshells. In addition, work is currently being done to investigate the potential for embedding drugs into the layers of the "two-layer" nanoshell for drug delivery. A more interesting approach would be to combine the photothermal treatments with drug delivery. A system could potentially be designed that would release its drug payload once the particle has been excited through NIR light, disrupting the layers on the nanoshell. These steps are the next logical progression towards developing a potent system for targeted cancer therapy.

LIST OF REFERENCES

(2013). Cancer Facts and Figures 2013. Atlanta, American Cancer Society.

(2013). "Pilot Study of AuroLase Therapy in Refractory and/or Recurrent Tumors of the Head and Neck,." from http://www.clinicaltrials.gov/ct2/show/NCT00848042.

(2013). "Soy PC." Retrieved 4/15/2013, 2013, from http://avantilipids.com/index.php?option=com_content&view=article&id=348&Itemid=212&catnumber=840054.

Alkilany, A. M. and C. J. Murphy (2010). "Toxicity and cellular uptake of gold nanoparticles: what we have learned so far?" Journal of Nanoparticle Research **12**(7): 2313-2333.

Duff, D. G., et al. (1993). "A New Hydrosol of Gold Clusters. 1. Formation and Particle-Size Variation." Langmuir **9**(9): 2301-2309.

England, C., et al. (in prep.) "Increased penetration into solid tumor tissue using two- and three-layered gold nanoparticles."

Frens, G. (1973). "Controlled Nucleation for Regulation of Particle Size in Monodisperse Gold Suspensions." Nature-Physical Science **241**(105): 20-22.

Gobin, A. M., et al. (2007). "Near-infrared resonant nanoshells for combined optical imaging and photothermal cancer therapy." Nano Letters **7**(7): 1929-1934.

Gobin, A. M., et al. (2010). "Near-Infrared-Resonant Gold/Gold Sulfide Nanoparticles as a Photothermal Cancer Therapeutic Agent." Small **6**(6): 745-752.

Goodman, C. M., et al. (2004). "Toxicity of Gold Nanoparticles Functionalized with Cationic and Anionic Side Chains." Bioconjugate Chemistry **15**(4): 897-900.

Hirsch, L. R., et al. (2006). "Metal nanoshells." Annals of Biomedical Engineering **34**(1): 15-22.

Hirsch, L. R., et al. (2003). "Nanoshell-mediated near-infrared thermal therapy of tumors under magnetic resonance guidance." Proceedings of the National Academy of Sciences of the United States of America **100**(23): 13549-13554.

Ito, Y., et al. (2000). "Assessment of heating effects in skin during continuous wave near infrared spectroscopy." Journal of Biomedical Optics **5**(4): 383-390.

Jiang, J., et al. (2006). "Influence of liver cancer on lipid and lipoprotein metabolism." Lipids in Health and Disease **5**(1): 4.

Kennedy, L. C., et al. (2011). "A New Era for Cancer Treatment: Gold-Nanoparticle-Mediated Thermal Therapies." Small **7**(2): 169-183.

Kimling, J., et al. (2006). "Turkevich Method for Gold Nanoparticle Synthesis Revisited." The Journal of Physical Chemistry B **110**(32): 15700-15707.

Kong, G., et al. (2000). "Hyperthermia enables tumor-specific nanoparticle delivery: Effect of particle size." Cancer Research **60**(16): 4440-4445.

Loo, C., et al. (2005). "Immunotargeted nanoshells for integrated cancer imaging and therapy." Nano Letters **5**(4): 709-711.

Lowery, A. R., et al. (2006). "Immunonanoshells for targeted photothermal ablation of tumor cells." International Journal of Nanomedicine **1**(2): 149-154.

Maeda, H. (2001). The enhanced permeability and retention (EPR) effect in tumor vasculature: The key role of tumor-selective macromolecular drug targeting. Advances in Enzyme Regulation, Vol 41. G. Weber. Oxford, Pergamon-Elsevier Science Ltd. **41:** 189-207.

Murphy, C. J., et al. (2008). "Gold Nanoparticles in Biology: Beyond Toxicity to Cellular Imaging." Accounts of Chemical Research **41**(12): 1721-1730.

O'Neal, D. P., et al. (2004). "Photo-thermal tumor ablation in mice using near infrared-absorbing nanoparticles." Cancer Letters **209**(2): 171-176.

Oldenburg, S. J., et al. (1998). "Nanoengineering of optical resonances." Chemical Physics Letters **288**(2-4): 243-247.

Oldenburg, S. J., et al. (1999). "Infrared extinction properties of gold nanoshells." Applied Physics Letters **75**(19): 2897-2899.

Stöber, W., et al. (1968). "Controlled growth of monodisperse silica spheres in the micron size range." Journal of Colloid and Interface Science **26**(1): 62-69.

Takahashi, H., et al. (2006). "Modification of gold nanorods using phospatidylcholine to reduce cytotoxicity." Langmuir **22**(1): 2-5.

Turkevich, J. (1985). "Colloidal gold. Part II." Gold Bulletin **18**(4): 125-131.

Turkevich, J., et al. (1951). "A study of the nucleation and growth processes in the synthesis of colloidal gold." Discussions of the Faraday Society **11**(0): 55-75.

van de Ven, A. L., et al. (2012). "Integrated intravital microscopy and mathematical modeling to optimize nanotherapeutics delivery to tumors." Aip Advances **2**(1).

Yen, J. C., et al. (1995). "A new criterion for automatic multilevel thresholding." IEEE Trans Image Process **4**(3): 370-378.

Zamboni, W. C., et al. (2012). "Best Practices in Cancer Nanotechnology: Perspective from NCI Nanotechnology Alliance." Clinical Cancer Research **18**(12): 3229-3241.

APPENDIX I: DARK-FIELD IMAGES

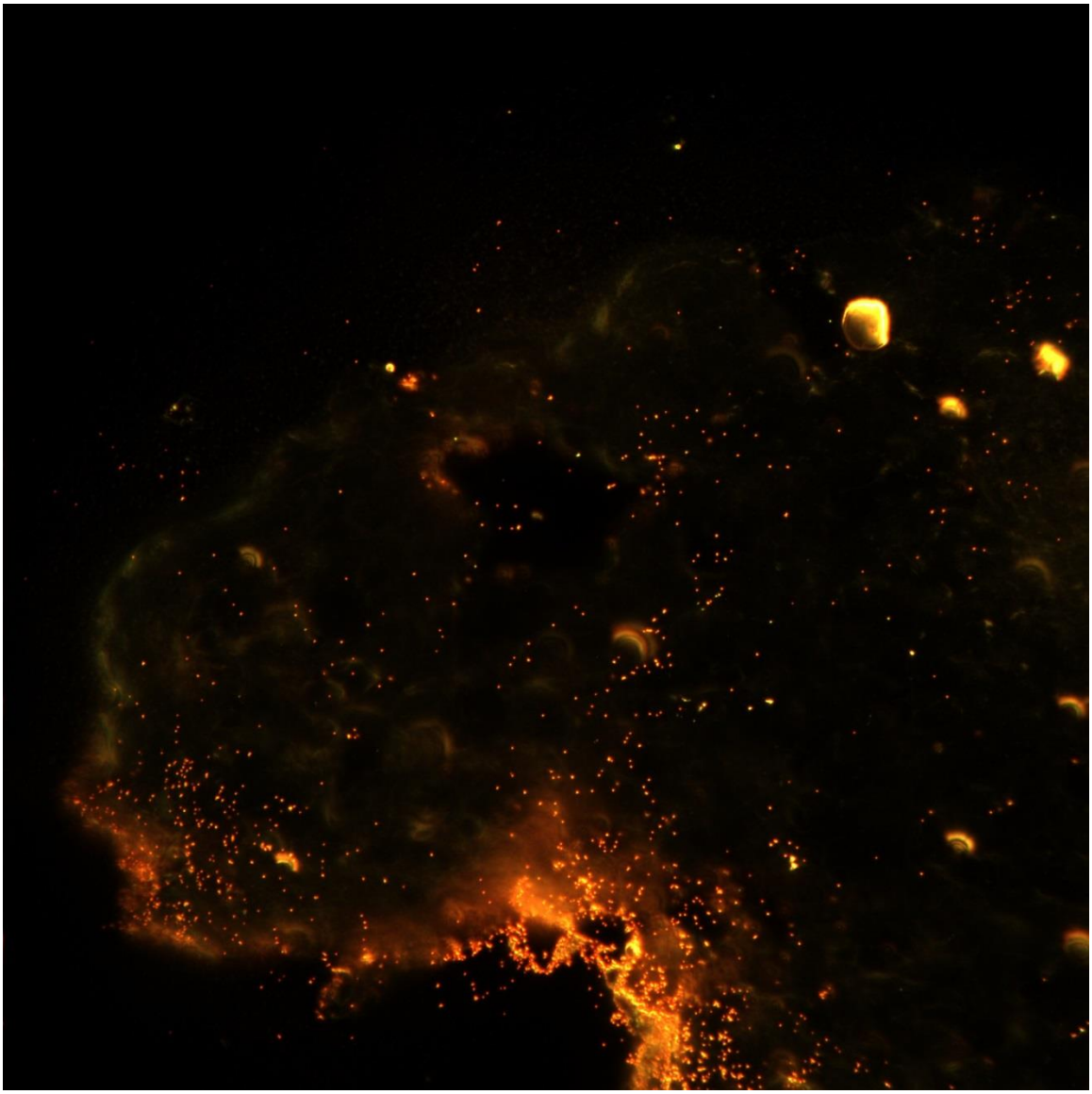

Figure 9 – A549 #1 Sample #2 Image #1

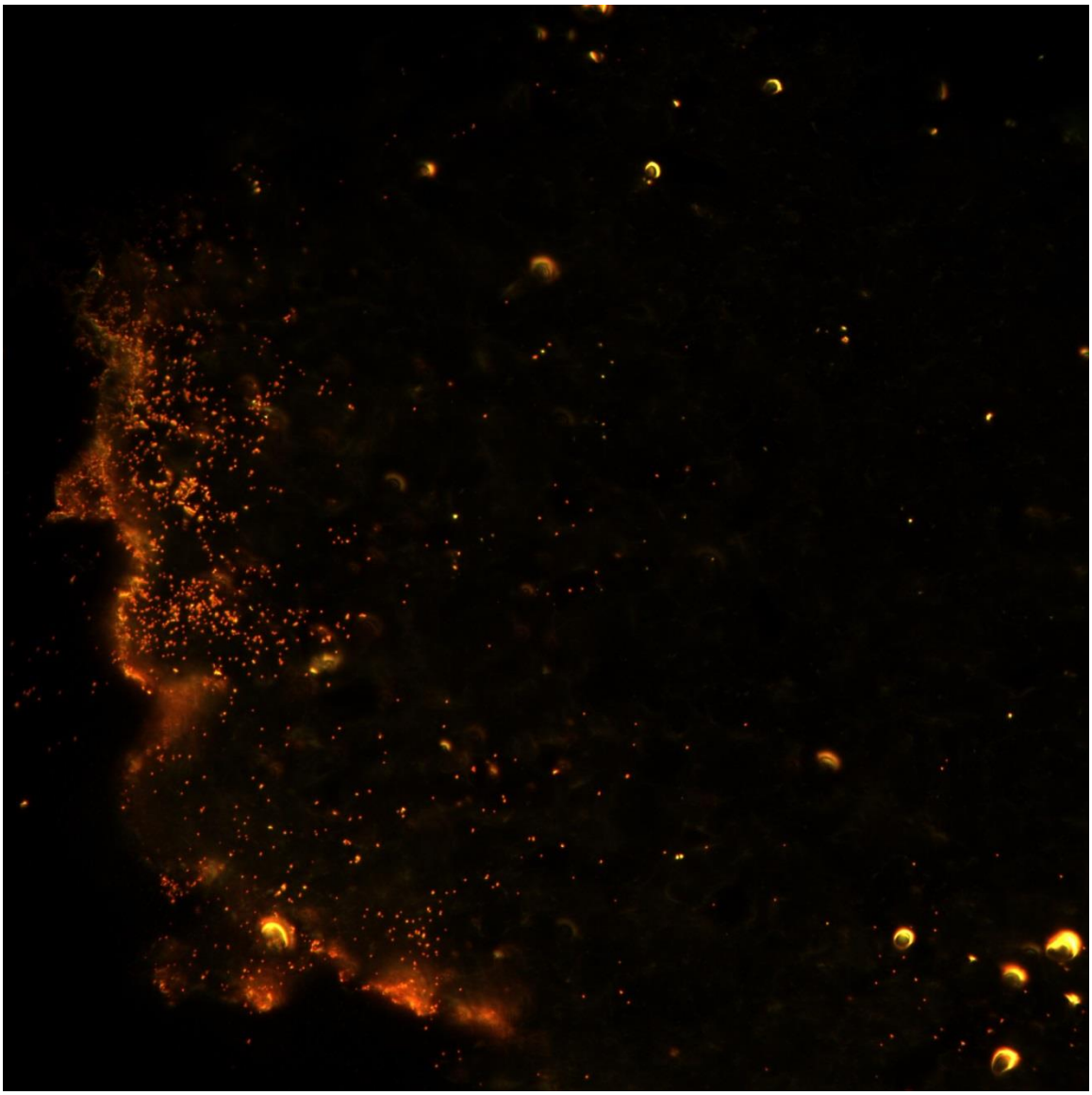

Figure 10 – A549 #1 Sample #2 Image #2

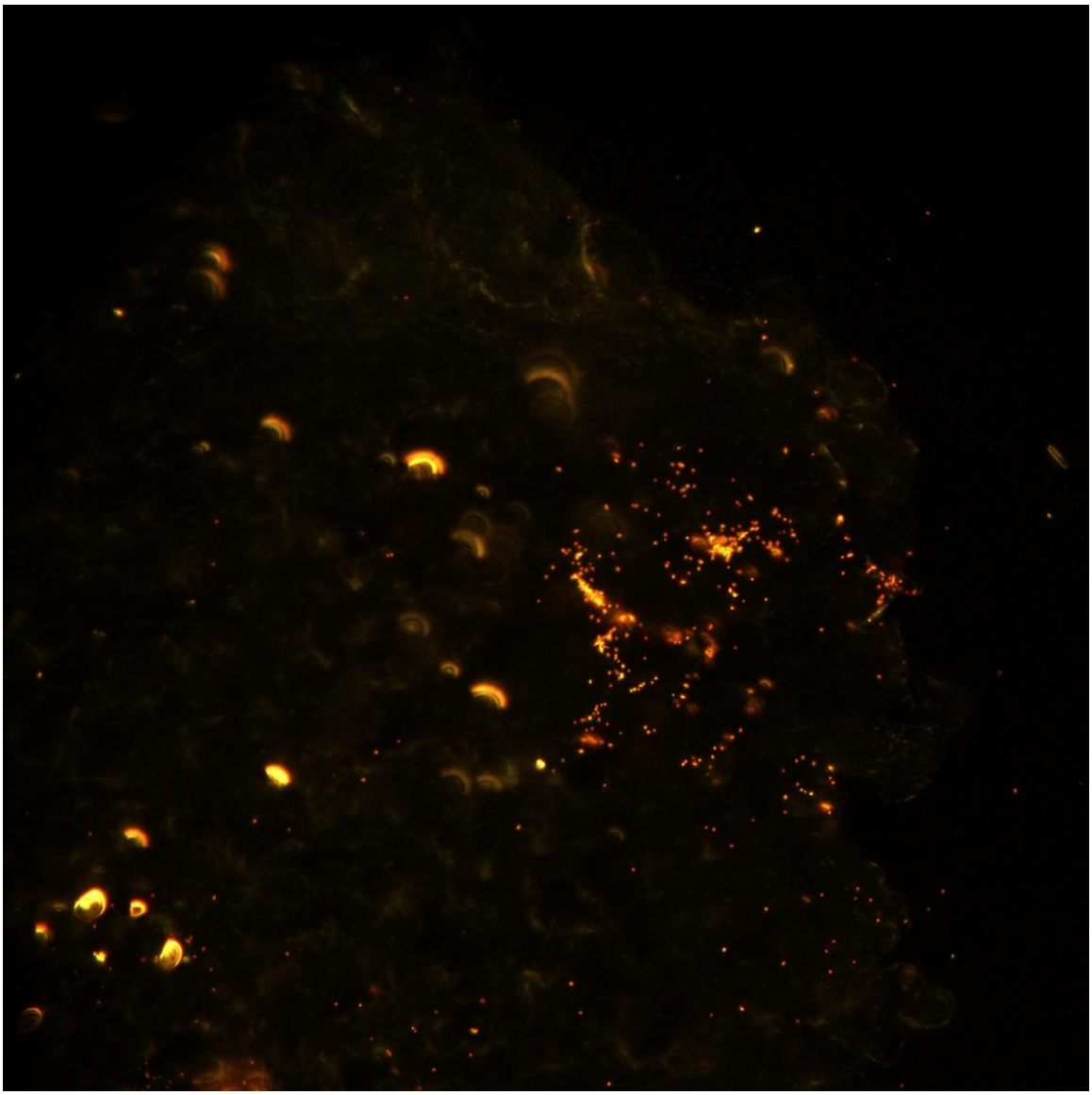

Figure 11 – A549 #1 Sample #2 Image #3

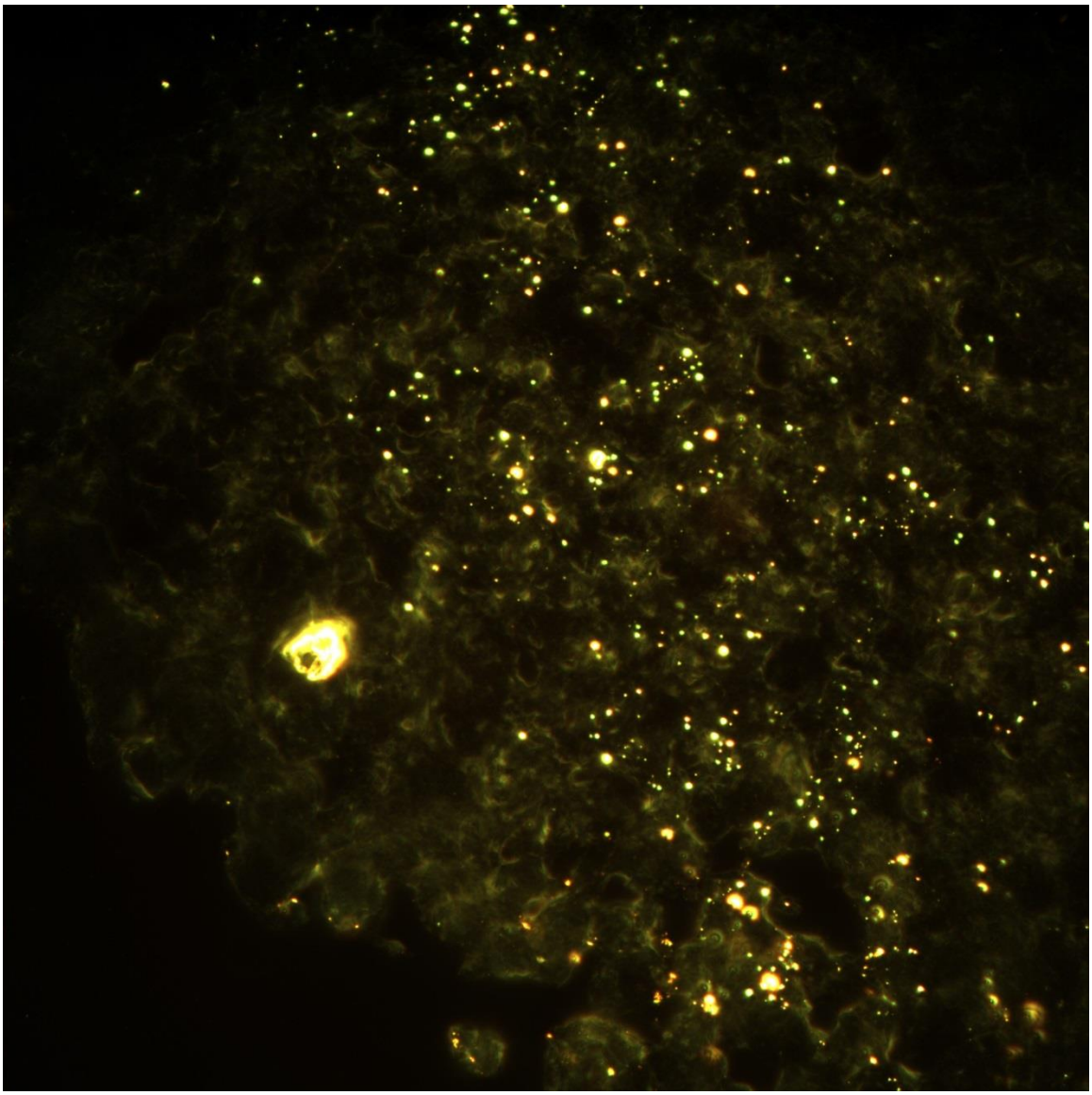

Figure 12 – A549 #5 Sample #1 Image #1

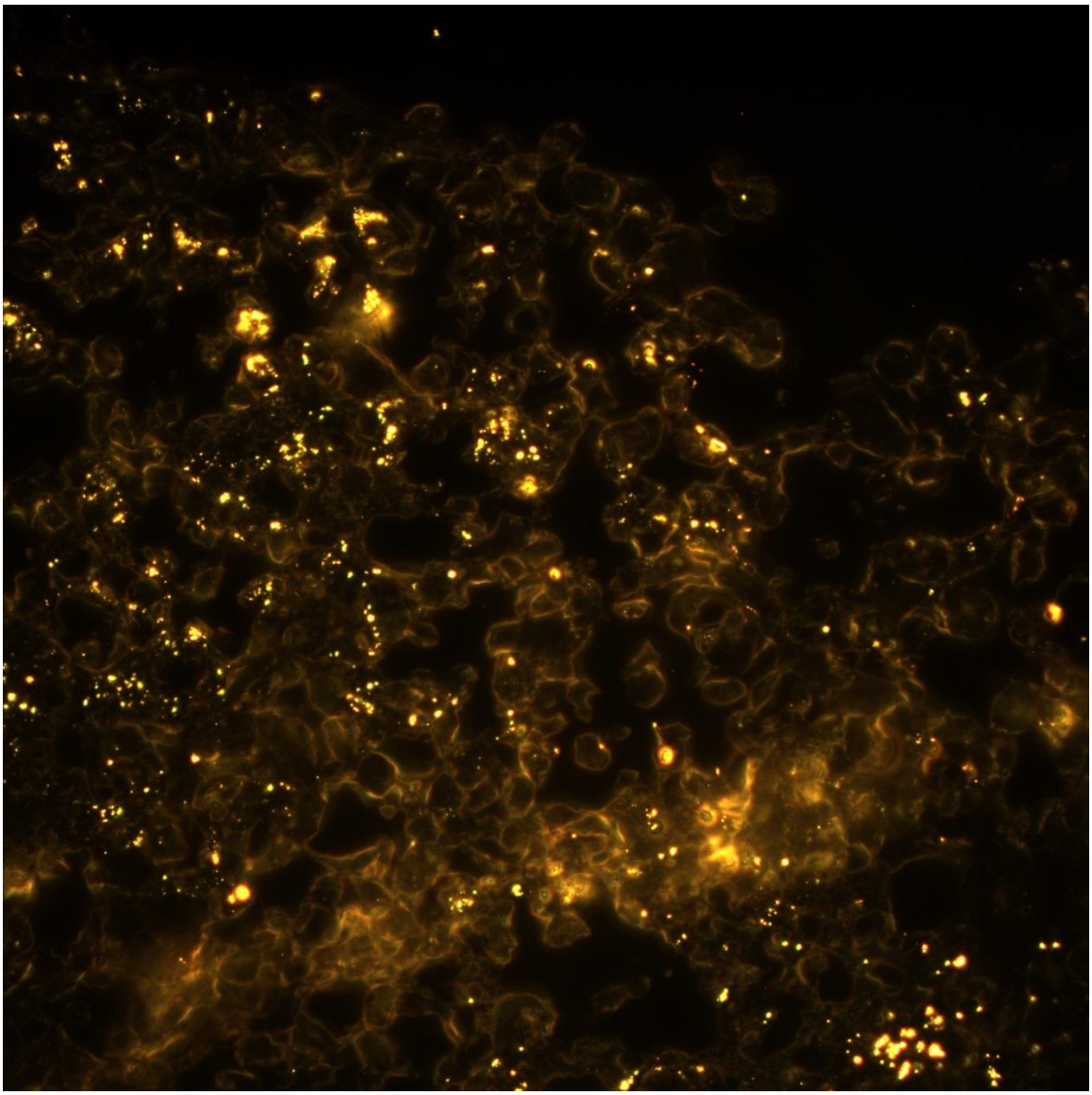

Figure 13 – HEPG2 tissue incubated with “two-layer” citrate-gold nanoparticles

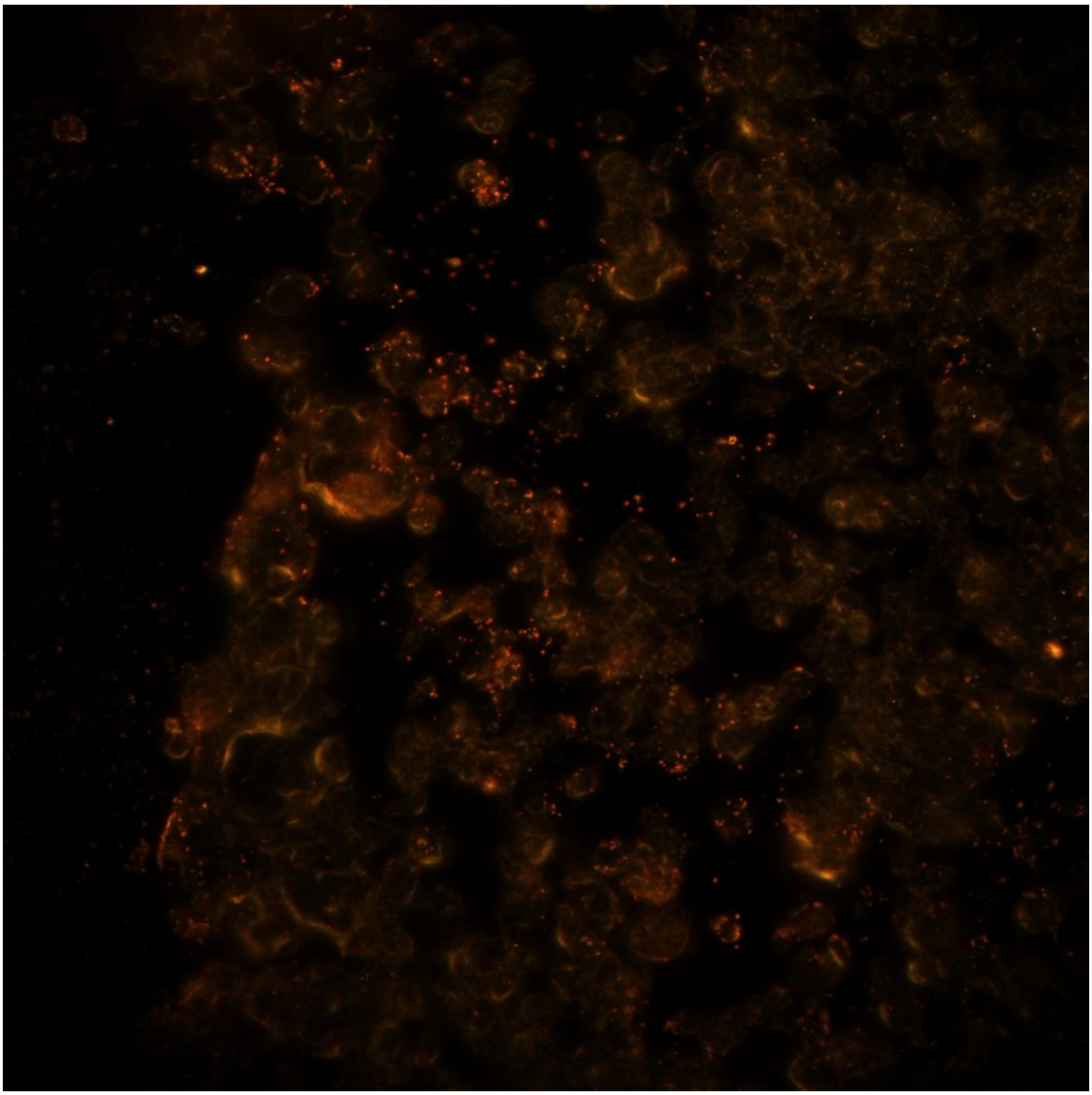

Figure 14 – HEPG2 tissue incubated with “three-layer” gold nanoshells

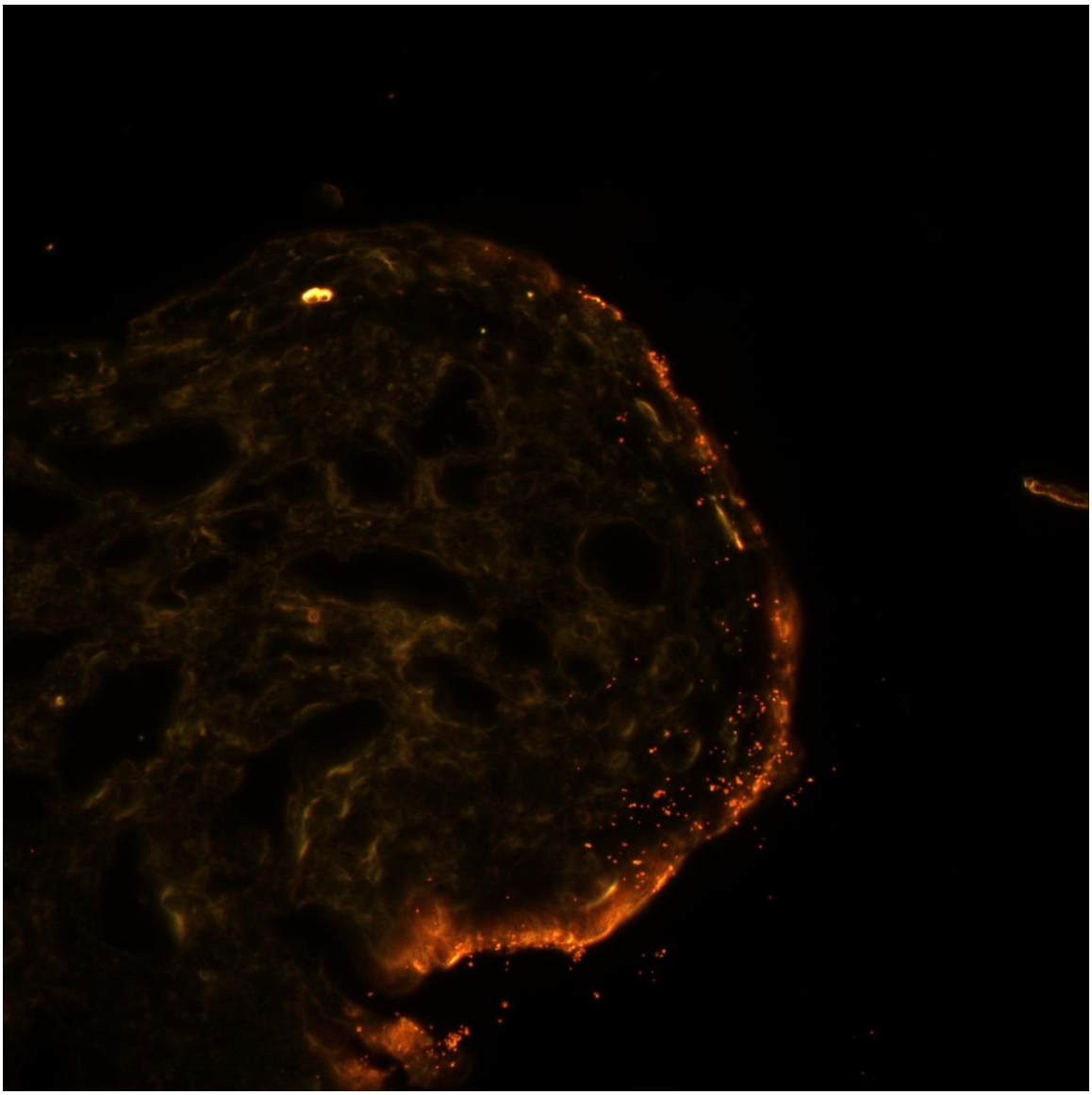

Figure 15- HEPG2 tissue incubated with “two-layer” gold nanoshells

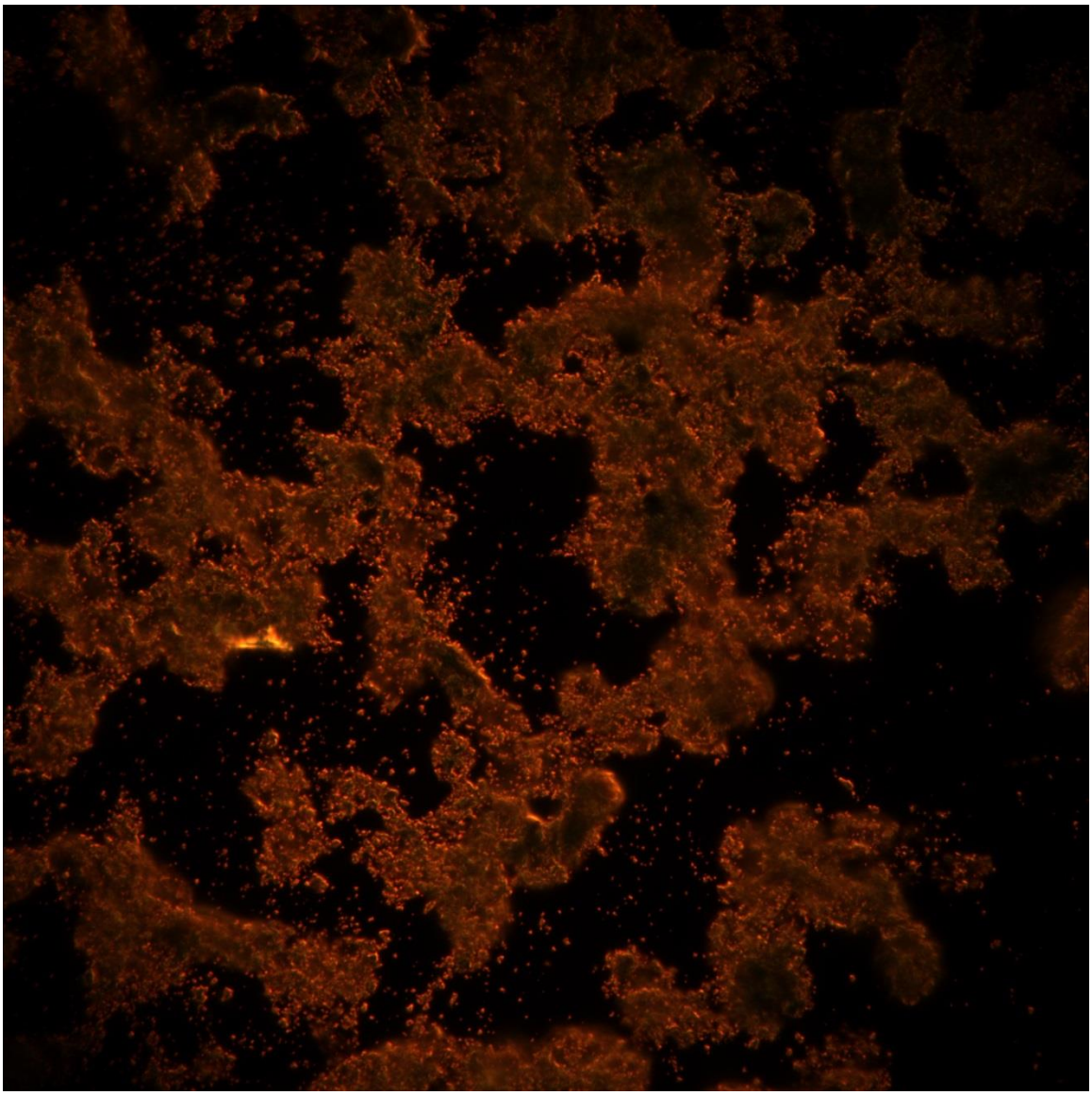

Figure 16 – S2VP10 tissue incubated with PEGylated gold nanoshells

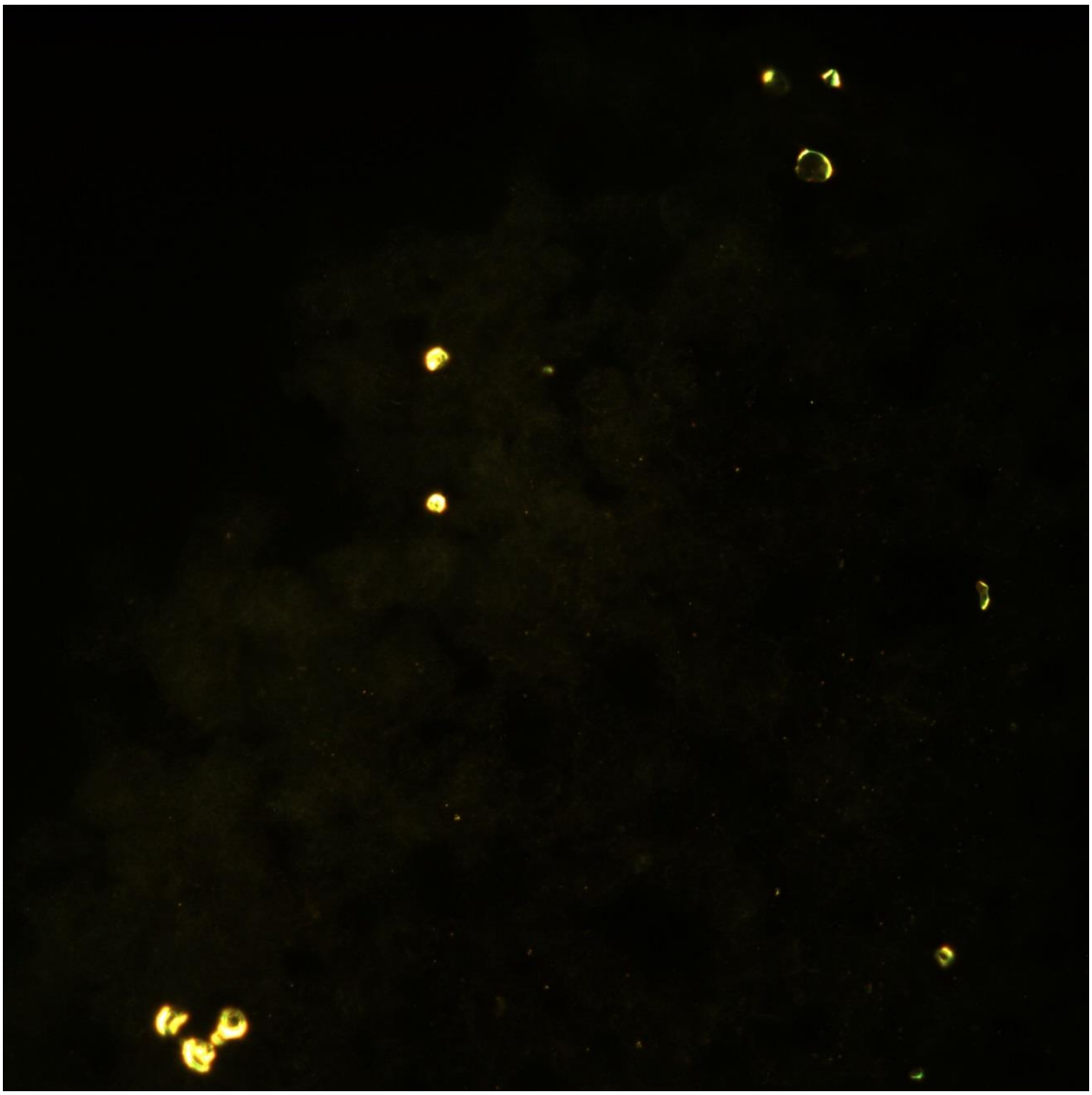

Figure 17 – S2VP10 tissue incubated with “two-layer” gold nanoshells

VITA

Thomas Priest received his Bachelor's of Science in Bioengineering with honors from the University of Louisville in 2012. While a student, he worked at Pacific Northwest National Laboratory as a technical intern. He worked with Julia Laskin, performing research on ultrasmall gold clusters. He gained valuable experience in nanomaterial synthesis as well as mass spectroscopy. The work with the Laskin group has resulted in several publications in academic journals. Currently, Thomas is completing a Master's of Engineering in Bioengineering at University of Louisville under Dr. Hermann Frieboes, and expects to graduate with honors.